

Doubly Enhanced Skyrmions in $\nu = 2$ Bilayer Quantum Hall States

Norio KUMADA*, Anju SAWADA, Zyun F. EZAWA, Satoshi NAGAHAMA,
 Hirofumi AZUHATA, Koji MURAKI¹, Tadashi SAKU¹ and Yoshiro HIRAYAMA¹

Department of Physics, Tohoku University, Sendai 980-8578

¹*NTT Basic Research Laboratories, 3-1 Morinosato-Wakamiya, Atsugi, Kanagawa 243-0198*

(Received July 12, 2000)

Skyrmion excitations were measured and compared for the first time in the bilayer quantum Hall (QH) state at the Landau-level filling factor $\nu = 2$ and in the monolayer QH state at $\nu = 1$. The observed number of flipped spins, N_{spin} , is 14 in the bilayer sample with a large tunnelling gap, and $N_{\text{spin}} = 7$ in the bilayer sample with a small tunnelling gap, while it is $N_{\text{spin}} = 7$ in the monolayer sample. The difference is interpreted to be due to the interlayer exchange interaction.

KEYWORDS: quantum Hall effect, semiconductor, magnetotransport, Skyrmion, exchange interactions

The bilayer quantum Hall (QH) state has attracted a great deal of recent attention, particularly at the Landau-level filling factor $\nu = 2$. At this filling factor, the competition between the tunnelling and the Zeeman effect leads to interesting physics. A phase transition has been observed between the spin-polarized state and the spin-unpolarized state, as revealed by magnetotransport measurements,^{1,2)} light-scattering spectroscopy^{3,4)} and capacitance spectroscopy.⁵⁾ The existence of interlayer coherence has been pointed out^{2,6)} in the $\nu = 2$ spin-unpolarized bilayer QH state. Moreover, some theoretical works suggest a new phase that is a canted antiferromagnetic state.⁷⁾ In the $\nu = 2$ spin-polarized bilayer QH state, electrons in each layer tend to configure the monolayer $\nu = 1$ QH state separately,¹⁾ which is referred to as the compound state. This state is realized when the electron density of each layer is equal and the total density n_t is sufficiently high.^{1,8)} It is important to explore whether there is any difference between the excitations in the compound $\nu = 2$ state and the simple monolayer $\nu = 1$ QH state, since it will yield deep insight into the role of the interlayer Coulomb and tunnelling interactions.

In the monolayer $\nu = 1$ QH state, the Coulomb interaction makes the excitation energy much larger than the expected single-particle Zeeman energy. Provided that the Zeeman effect is small, the lowest-energy-charged excitations are spin textures known as Skyrmions.⁹⁻¹⁷⁾ They are characterized by the number of flipped spins, N_{spin} . N_{spin} is determined from the measurements of the activation energy by tilting a sample in the magnetic field while keeping the perpendicular component B_{\perp} fixed. The in-plane magnetic field B_{\parallel} couples to the system only through the Zeeman energy. The dependence of the excitation energy Δ on the total magnetic field B_{tot} is

$$\Delta = \Delta_{0,s}(B_{\perp}) + N_{\text{spin}}|g^*|\mu_B B_{\text{tot}}. \quad (1)$$

The activation energy Δ is determined from the tem-

perature dependence of the magnetoresistance: $R_{xx} = R_0 \exp(-\Delta/2T)$. The first term, $\Delta_{0,s}$, is the contribution to the gap from the non-Zeeman effect such as the Coulomb interaction, and usually depends on the impurity concentration. Here, g^* is the gyromagnetic ratio ($g^* = -0.46$ in GaAs) and μ_B is the Bohr magneton. From this equation, N_{spin} is determined by $\partial\Delta/\partial(|g^*|\mu_B B_{\text{tot}})$. N_{spin} decreases as the total field increases,¹²⁾ because the Skyrmion size becomes smaller.

In this Letter, we investigate Skyrmion excitations in the compound $\nu = 2$ state. Because a compound state is composed of two independent monolayer states, the tunnelling gap collapses, and spin excitations can be analyzed by eq. (1). We compare the activation energy of the bilayer $\nu = 2$ QH state in the samples with different tunnelling energy gaps Δ_{SAS} with that of the induced monolayer $\nu = 1$ QH state. Here, the induced monolayer state is constructed by emptying the electrons in one layer (the experimental technique is explained in next paragraph) in the same double quantum well sample.

Three samples with different barrier heights but the same barrier width were grown by molecular-beam epi-

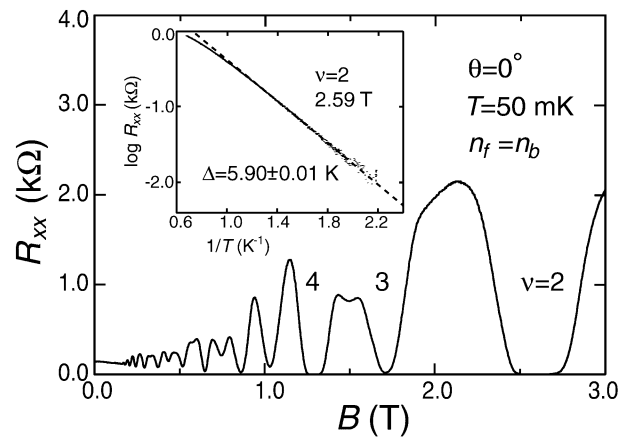


Fig. 1. R_{xx} vs B at $\theta = 0^\circ$ in sample #10.9 with $n_t = 1.2 \times 10^{11} \text{ cm}^{-2}$ at the balanced point. The inset shows an Arrhenius plot of the magnetoresistance at $\nu = 2$ ($B_{\perp} = 2.59 \text{ T}$).

* E-mail: kumada@mail.cc.tohoku.ac.jp

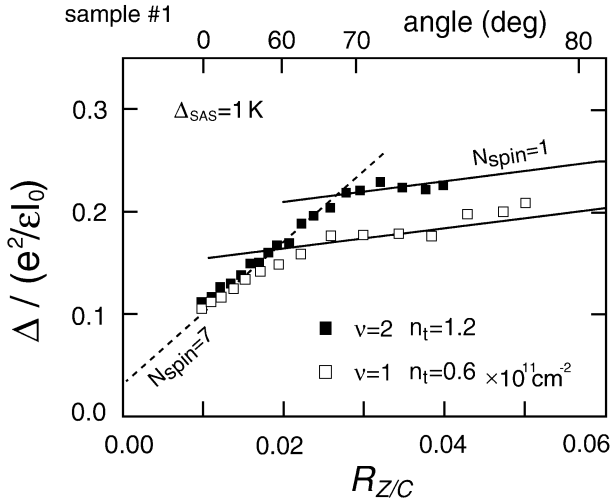


Fig. 2. The activation energy by tilting sample #1 of the $\nu = 1$ and $\nu = 2$ QH states as a function of the normalized Zeeman energy $R_{Z/C}$ with $e^2/\epsilon\ell_0 = 81.7$ K. The corresponding tilt angles are indicated on the top axis. The solid squares are for the bilayer $\nu = 2$ QH state at the balanced point ($n_f = n_b$). The open squares are for the induced monolayer $\nu = 1$ QH state. For comparison, we have drawn lines $N_{\text{spin}} = 7$ (dashed) and $N_{\text{spin}} = 1$ (solid).

taxy. They consist of two GaAs quantum wells of 200 Å width separated by a 31-Å-thick barrier of $\text{Al}_x\text{Ga}_{1-x}\text{As}$ ($x = 0.3, 0.33$ and 1). We label them #10.9, #7.6 and #1 according to their $\Delta_{\text{SAS}} = 10.9$ K, 7.6 K and 1 K, respectively. (Δ_{SAS} of the highest barrier sample cannot be determined by the Shubnikov-de Hass measurement. We estimate $\Delta_{\text{SAS}} = 1$ K using a self-consistent calculation.) The unique structure of samples #10.9 and #1 is that the modulation doping is carried out only on the front layer, and the back-layer electron is fully field-induced through an n^+ -GaAs layer acting as a back gate.¹⁸) Hence, one can control the electron density of the back layer n_b from 0 to $1.2 \times 10^{11} \text{ cm}^{-2}$ by adjusting the back gate bias from 0 to 1.2 V, while the electron density of the front layer n_f is controlled by adjusting a Ti/Au front Schottky gate bias. This sample structure enables us to easily realize the balanced bilayer system ($n_f = n_b$) and the monolayer system ($n_f \neq 0, n_b = 0$). On the other hand, the modulation doping is carried out on both layers in sample #7.6. The low-temperature mobility of samples #10.9 and #1 is $2 \times 10^6 \text{ cm}^2/\text{Vs}$ with the electron density of $2 \times 10^{11} \text{ cm}^{-2}$, while that of sample #7.6 is $0.3 \times 10^6 \text{ cm}^2/\text{Vs}$ with the electron density of $2.6 \times 10^{11} \text{ cm}^{-2}$.

Measurements were performed with the samples mounted in a mixing chamber of a dilution refrigerator. The magnetic field of maximum 13.5 T was applied to the samples. Standard low-frequency ac lock-in techniques were used with a current of 20 nA to avoid heating effects. The samples mounted on a goniometer with a superconducting stepper motor¹⁹) rotate in any direction in the magnetic field in units of 0.05°. Figure 1 shows the magnetoresistance R_{xx} as a function of B . In the inset, we show the typical temperature dependence of the magnetoresistance and obtain the activation energy from the slope of the least-squares fit.

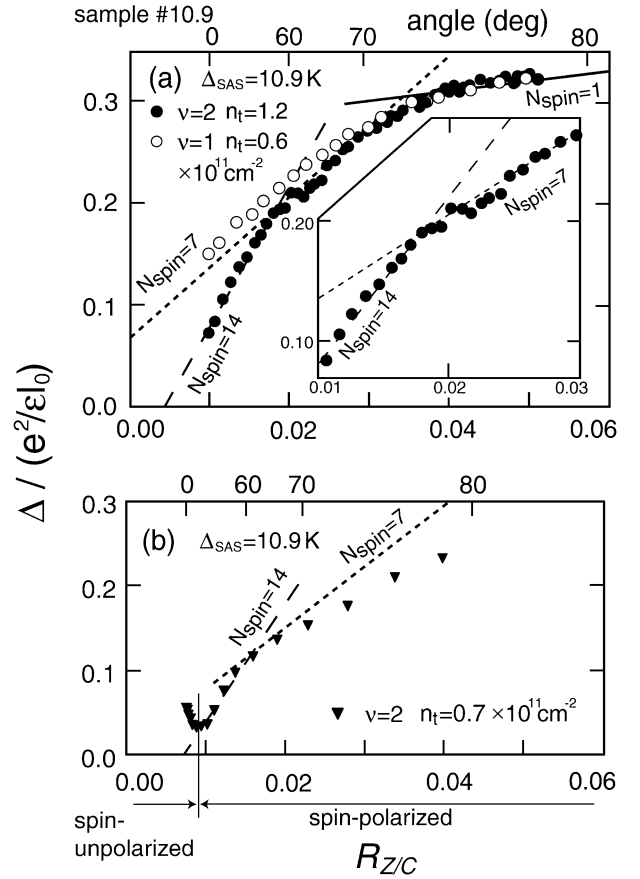


Fig. 3. The activation energy by tilting sample #10.9 of the $\nu = 1$ and $\nu = 2$ QH states as a function of the normalized Zeeman energy $R_{Z/C}$ with $e^2/\epsilon\ell_0 = 81.7$ K. The solid marks are for the bilayer $\nu = 2$ QH state at the balanced point. The open marks are for the induced monolayer $\nu = 1$ QH state. (The inset shows the data of the bilayer $\nu = 2$ QH state around the inflection point from $N_{\text{spin}} = 14$ to $N_{\text{spin}} = 7$). For comparison, we have drawn lines $N_{\text{spin}} = 14$ (long-dashed), 7 (dashed) and 1 (solid). In (b), a spin-polarized (compound) state is realized for $R_{Z/C} \geq 0.009$ with $e^2/\epsilon\ell_0 = 62.5$ K.

Figure 2 presents the results of measurements by tilting sample #1 with a small tunnelling gap ($\Delta_{\text{SAS}} = 1$ K). The activation energy divided by the Coulomb energy is plotted vs the Zeeman energy divided by the Coulomb energy $R_{Z/C} = |g^*|\mu_B B_{\text{tot}}/(e^2/\epsilon\ell_0)$, where $\ell_0 = \sqrt{\hbar/eB_{\perp}}$ is the magnetic length. We used the dielectric constant $\epsilon = 12.9$. Each data set starts from the magnetic field normal to the two-dimensional plane ($B_{\text{tot}} = B_{\perp}$). As Fig. 2 shows, in the $\nu = 2$ data at $n_t = 1.2 \times 10^{11} \text{ cm}^{-2}$, the activation energy initially rises quickly as the total magnetic field increases, where N_{spin} is found to be about 7. At $R_{Z/C} = 0.027$, the slope changes suddenly and we obtain about $N_{\text{spin}} = 1$ for $R_{Z/C} \geq 0.027$. The induced monolayer $\nu = 1$ data at $n_t = 0.6 \times 10^{11} \text{ cm}^{-2}$ share all of these properties except for the inflection point.

Figure 3 presents the results of measurements by tilting sample #10.9 with a large tunnelling gap ($\Delta_{\text{SAS}} = 10.9$ K). From the $\nu = 2$ data at $n_t = 1.2 \times 10^{11} \text{ cm}^{-2}$ in Fig. 3(a), $N_{\text{spin}} = 14$ (least-squares fitting value: 14.0 ± 0.5) is derived for $R_{Z/C} \leq 0.018$. N_{spin} changes from 14 to 7 at $R_{Z/C} = 0.018$, and finally changes to 1

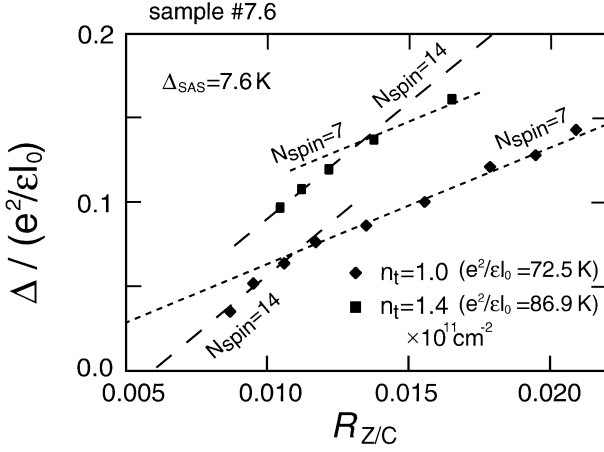


Fig. 4. The activation energy by tilting sample #7.6 of the $\nu = 2$ QH states at the balanced point as a function of the normalized Zeeman energy $R_{Z/C}$. For comparison, we have drawn lines $N_{\text{spin}} = 14$ (long-dashed) and 7 (dashed).

at $R_{Z/C} = 0.033$. In contrast, the induced monolayer $\nu = 1$ data at $n_t = 0.6 \times 10^{11} \text{ cm}^{-2}$ show $N_{\text{spin}} = 7$ (7.3 ± 0.4) for $R_{Z/C} \leq 0.018$, as observed in sample #1 at the same $R_{Z/C}$ value. It should be emphasized that $N_{\text{spin}} = 14$ is twice as large as $N_{\text{spin}} = 7$.

So far, we have focused on the spin-polarized (compound) state at $\nu = 2$, which is realized at higher density. We now study the state at $\nu = 2$ at low density, which is a spin-unpolarized state.⁸⁾ When the sample is tilted, the data at $\nu = 2$ with $n_t = 0.7 \times 10^{11} \text{ cm}^{-2}$ in Fig. 3(b) show a rapid decrease to the limit of $R_{Z/C} = 0.009$, as in the bilayer $\nu = 1$ QH state,²⁰⁾ which indicates that interlayer coherence spontaneously developed in the $\nu = 2$ QH state.²⁾ The other feature for the $\nu = 2$ QH state is that it starts to increase at $R_{Z/C} = 0.009$. The behavior of the activation energy for $R_{Z/C} \geq 0.009$ is unique to the compound $\nu = 2$ state.²¹⁾ Namely, the state is stable only at the balanced point and the activation energy increases as the sample is tilted. Consequently, we have two phases²¹⁾ with the phase transition at $R_{Z/C} = 0.009$. It has been interpreted^{21, 22)} that a phase transition occurs from the spin-unpolarized (coherent) state to the spin-polarized (compound) state, because Δ_{SAS} decreases effectively as B_{\parallel} increases.²³⁾ Once in the compound state, the tunnelling gap collapses and N_{spin} can be determined by eq. (1). In this compound state, we have derived about $N_{\text{spin}} = 14$ at $0.009 \leq R_{Z/C} \leq 0.018$, but N_{spin} at higher $R_{Z/C}$ is slightly less than 7.

In Fig. 4, we show the data of sample #7.6 ($\Delta_{\text{SAS}} = 7.6 \text{ K}$), whose mobility, $0.3 \times 10^6 \text{ cm}^2/\text{Vs}$, is one order lower than that of sample #10.9. These data are consistent with those in sample #10.9.

It is essential to compare the compound $\nu = 2$ state at $n_t = 1.2 \times 10^{11} \text{ cm}^{-2}$ to the monolayer $\nu = 1$ QH state at $n_t = 0.6 \times 10^{11} \text{ cm}^{-2}$. We have tuned the density so that this compound $\nu = 2$ state is composed of two monolayer $\nu = 1$ states at $n_t = 0.6 \times 10^{11} \text{ cm}^{-2}$. On one hand, in sample #1 (Fig. 2) with $\Delta_{\text{SAS}} = 1 \text{ K}$, the excitation with $N_{\text{spin}} = 7$ was observed both in the compound $\nu = 2$ state and in the induced monolayer $\nu = 1$ QH state. On

the other hand, in sample #10.9 (Fig. 3) with $\Delta_{\text{SAS}} = 10.9 \text{ K}$, the excitation with $N_{\text{spin}} = 14$ was observed in the compound $\nu = 2$ state at $R_{Z/C} \leq 0.018$, but $N_{\text{spin}} = 7$ in the induced monolayer $\nu = 1$ QH state. On the basis of these results, it is reasonable to conclude that the excitation with $N_{\text{spin}} = 14$ ($N_{\text{spin}} = 7$) occurs when the tunnelling interaction is large (small).

Let us elucidate the difference in spin excitations in these two samples with small and large tunnelling effects. Note that the difference does not originate in the direct interlayer Coulomb interaction since it is identical between the two samples. The monolayer $\nu = 1$ QH state is a QH ferromagnet, where all spins are aligned in a single direction not only by the Zeeman effect but also by the intralayer Coulomb exchange interaction. We now consider the compound $\nu = 2$ state, which is composed of two monolayer QH ferromagnets. The two layers are independent when the tunnelling effect is absent. Hence, we obtain spin excitations identical to those in the monolayer QH state in sample #1. However, a large tunnelling effect implies a large overlap of the wave functions, which makes the interlayer exchange interaction operate. Consequently, a spin flip in one of the layers affects the spin texture in the other layer. It is reasonable to expect that Skyrmions are doubly created on the two layers in sample #10.9 due to the interlayer exchange interaction. It is intriguing to consider whether the interlayer exchange interaction induces the ferromagnetic or antiferromagnetic interaction. The former enhances a Skyrmion-Skyrmion pair (Fig. 5). The mechanism is akin to that in the $\nu = 2$ interlayer-coherent phase, where the experimental data¹⁾ is interpreted by a pair excitation of Skyrmions.⁶⁾ On the other hand, an antiferromagnetic interaction^{24, 25)} will enhance a Skyrmion-anti-Skyrmion pair. However, the present magnetotransport experiment is unable to determine the type of the interaction.

It is notable that the spin flip makes a transition from $N_{\text{spin}} = 14$ to 7 at $R_{Z/C} = 0.018$ in Fig. 3(a). The flip number for $R_{Z/C} \geq 0.018$ is identical ($N_{\text{spin}} = 7$) to the one in the induced monolayer QH state. This is presumably because the increase of the Zeeman energy overcomes the interlayer exchange interaction and Skyrmions are excited independently in each layer.

The energy and the size of the Skyrmion are theoretically estimated at $\nu = 1$ as^{9, 10, 26)}

$$\frac{\Delta}{e^2/\epsilon l_0} \simeq \sqrt{\frac{\pi}{32}} + \frac{3\beta}{4\kappa} - \Gamma_{\text{offset}} \quad (2)$$

where β represents the strength of the Coulomb energy which depends on sample parameters such as the layer thickness ($\beta = 3\pi^2/64$ for a large Skyrmion in an ideal planer system), and κ is the size of the Skyrmion

$$\kappa \simeq \frac{\beta^{1/3}}{2} \left\{ R_{Z/C} \ln \left(\frac{\sqrt{2\pi}}{32R_{Z/C}} + 1 \right) \right\}^{-1/3}. \quad (3)$$

The offset Γ_{offset} may be due to impurities in the sample. $N_{\text{spin}} = \partial(\Delta/(e^2/\epsilon l_0))/\partial R_{Z/C}$ depends smoothly on $R_{Z/C}$. The monolayer data of Schmeller *et al.*¹²⁾ are fitted reasonably well.⁶⁾

It is better to fit our experimental data by the lines

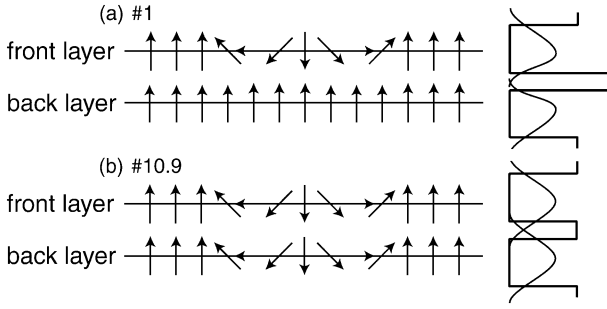


Fig. 5. Schematic diagram of spin flips in the compound $\nu = 2$ state. Arrows represent the direction of a spin. (a) In sample #1 with a small tunnelling gap, spin excitations are identical to those in the monolayer $\nu = 1$ QH state. (b) In sample #10.9 with a large tunnelling gap, spin excitations in one of the layers affect those in the other layer due to the interlayer exchange interaction. A Skyrmion-Skyrmion pair will be excited if the interaction is ferromagnetic. We have illustrated the overlap of the wave functions on the right-hand side.

$N_{\text{spin}} = 14, 7, 1$, not by this formula. This finding implies that at the preferred numbers $N_{\text{spin}} = 14, 7, 1$, the excitation occurs with lower energy than at other N_{spin} values. The same behavior is observed in samples with very different mobility ($2 \times 10^6 \text{ cm}^2/\text{Vs}$ and $0.3 \times 10^6 \text{ cm}^2/\text{Vs}$). Because of this finding, the preferred number is not due to the impurity effect. It must have a different origin, reminiscent of the magic-number momentum in a quantum-dot system where electrons configure in a polygonal pattern originating from the Coulomb interaction.^{27, 28} It is plausible that the non-Zeeman term $\Delta_{0,s}(B_{\perp})$ of the activation energy creates a local minimum at these preferred numbers to make a virtual Wigner crystal locally. Further experiments are needed to confirm this conjecture. It is intriguing that sudden changes in N_{spin} have also been observed in other experiments.¹⁵⁻¹⁷

In conclusion, we have measured the activation energy of the $\nu = 2$ QH state at the balanced point ($n_f = n_b$) and the $\nu = 1$ QH state at the monolayer point ($n_f \neq 0$, $n_b = 0$) by tilting the samples. We used three samples with different Δ_{SAS} and mobility. In samples #10.9 and #7.6, the excitation with $N_{\text{spin}} = 14$ was observed in the compound $\nu = 2$ state, which is twice as large as $N_{\text{spin}} = 7$ observed in the induced monolayer $\nu = 1$ QH state. In sample #1, in contrast, N_{spin} is the same in the compound $\nu = 2$ state and in the induced monolayer $\nu = 1$ QH state. We have argued that this difference is due to the interlayer exchange interaction.

We are grateful to H. Aoki for useful discussions. This research was supported in part by Grants-in-Aid for Scientific Research from the Ministry of Education, Science, Sports and Culture (Nos. 10203201, 10640244, 11125203, 11304019), the Mitsubishi Foundation, CREST-JST and

NEDO “NTDP-98” projects.

- 1) A. Sawada, Z. F. Ezawa, H. Ohno, Y. Horikoshi, Y. Ohno, S. Kishimoto, F. Matsukura, M. Yasumoto and A. Urayama: Phys. Rev. Lett. **80** (1998) 4534.
- 2) A. Sawada, Z. F. Ezawa, H. Ohno, Y. Horikoshi, A. Urayama, Y. Ohno, S. Kishimoto, F. Matsukura and N. Kumada: Phys. Rev. B **59** (1999) 14888.
- 3) V. Pellegrini, A. Pinczuk, B. S. Dennis, A. S. Plaut, L. N. Pfeiffer and K. W. West: Phys. Rev. Lett. **78** (1997) 310.
- 4) V. Pellegrini, A. Pinczuk, B. S. Dennis, A. S. Plaut, L. N. Pfeiffer and K. W. West: Science **281** (1998) 799.
- 5) V. S. Khrapai, E. V. Deviatov, A. A. Shashkin, V. T. Dolgoplov, F. Hastreiter, A. Wixforth, K. L. Campman and A. C. Gossard: Phys. Rev. Lett. **84** (2000) 725.
- 6) Z. F. Ezawa: Phys. Rev. Lett. **82** (1999) 3512.
- 7) L. Zheng, R. J. Radtke and S. Das Sarma: Phys. Rev. Lett. **78** (1997) 2453.
- 8) Z. F. Ezawa, A. Sawada, K. Muraki and Y. Hirayama: Physica E **7** (1999) 640.
- 9) S. L. Sondhi, A. Karlhede, S. A. Kivelson and E. H. Rezayi: Phys. Rev. B **47** (1993) 16419.
- 10) H. A. Fertig, L. Brey, R. Côté and A. H. MacDonald: Phys. Rev. B **50** (1994) 11018.
- 11) S. E. Barrett, G. Dabbagh, L. N. Pfeiffer, K. W. West and R. Tycko: Phys. Rev. Lett. **74** (1995) 5112.
- 12) A. Schmeller, J. P. Eisenstein, L. N. Pfeiffer and K. W. West: Phys. Rev. Lett. **75** (1995) 4290.
- 13) E. H. Aifer, B. B. Goldberg and D. A. Broido: Phys. Rev. Lett. **76** (1996) 680.
- 14) V. Bayot, E. Grivei, S. Melinte, M. B. Santos and M. Shayegan: Phys. Rev. Lett. **76** (1996) 4584.
- 15) D. K. Maude, M. Potemski, J. C. Portal, M. Henini, L. Eaves, G. Hill and M. A. Pate: Phys. Rev. Lett. **77** (1996) 4604.
- 16) R. J. Nicholas, D. R. Leadley, D. K. Maude, J. C. Portal, J. J. Harris and C. T. Foxon: Physica B **246** (1998) 1.
- 17) S. Melinte, E. Grivei, V. Bayot and M. Shayegan: Phys. Rev. Lett. **82** (1999) 2764.
- 18) K. Muraki, N. Kumada, T. Saku and Y. Hirayama: Jpn. J. Appl. Phys. **39** (2000) 2444.
- 19) M. Suzuki, A. Sawada, A. Ishiguro and K. Maruya: Cryogenics **37** (1997) 275.
- 20) S. Q. Murphy, J. P. Eisenstein, G. S. Boebinger, L. N. Pfeiffer and K. W. West: Phys. Rev. Lett. **72** (1994) 728.
- 21) A. Sawada, Z. F. Ezawa, H. Ohno, Y. Horikoshi, N. Kumada, Y. Ohno and S. Kishimoto: Physica E **7** (1999) 4604.
- 22) M. F. Yang and M. C. Chang: Phys. Rev. B **60** (1999) 13985.
- 23) J. Hu and A. H. MacDonald: Phys. Rev. B **46** (1992) 12554.
- 24) S. Das Sarma, S. Sachdev and L. Zheng: Phys. Rev. Lett. **79** (1997) 917.
- 25) B. Paredes, C. Tejedor, L. Brey and L. M. Moreno: Phys. Rev. Lett. **83** (1999) 2250.
- 26) Z. F. Ezawa and K. Sasaki: J. Phys. Soc. Jpn. **68** (1999) 576.
- 27) T. Seki, Y. Kuramoto and T. Nishino: J. Phys. Soc. Jpn. **65** (1996) 3945.
- 28) P. A. Maksym: Phys. Rev. B **53** (1996) 10871.

Note added in proof—The value of the gyromagnetic ratio $g^* = -0.46$ is only appropriate in zero magnetic field for bulk GaAs [M. Seck, M. Potemski and P. Wyder, Phys. Rev. B **56** (1997) 7422]. The magnetic field effect tends to linearly reduce the value of g [M. Dohers, K. v. Klitzing and G. Weimann, Phys. Rev. B **38** (1988) 5453]. For our case this effect increases slightly the deduced Skyrmion number, but it does not change our conclusion at all.